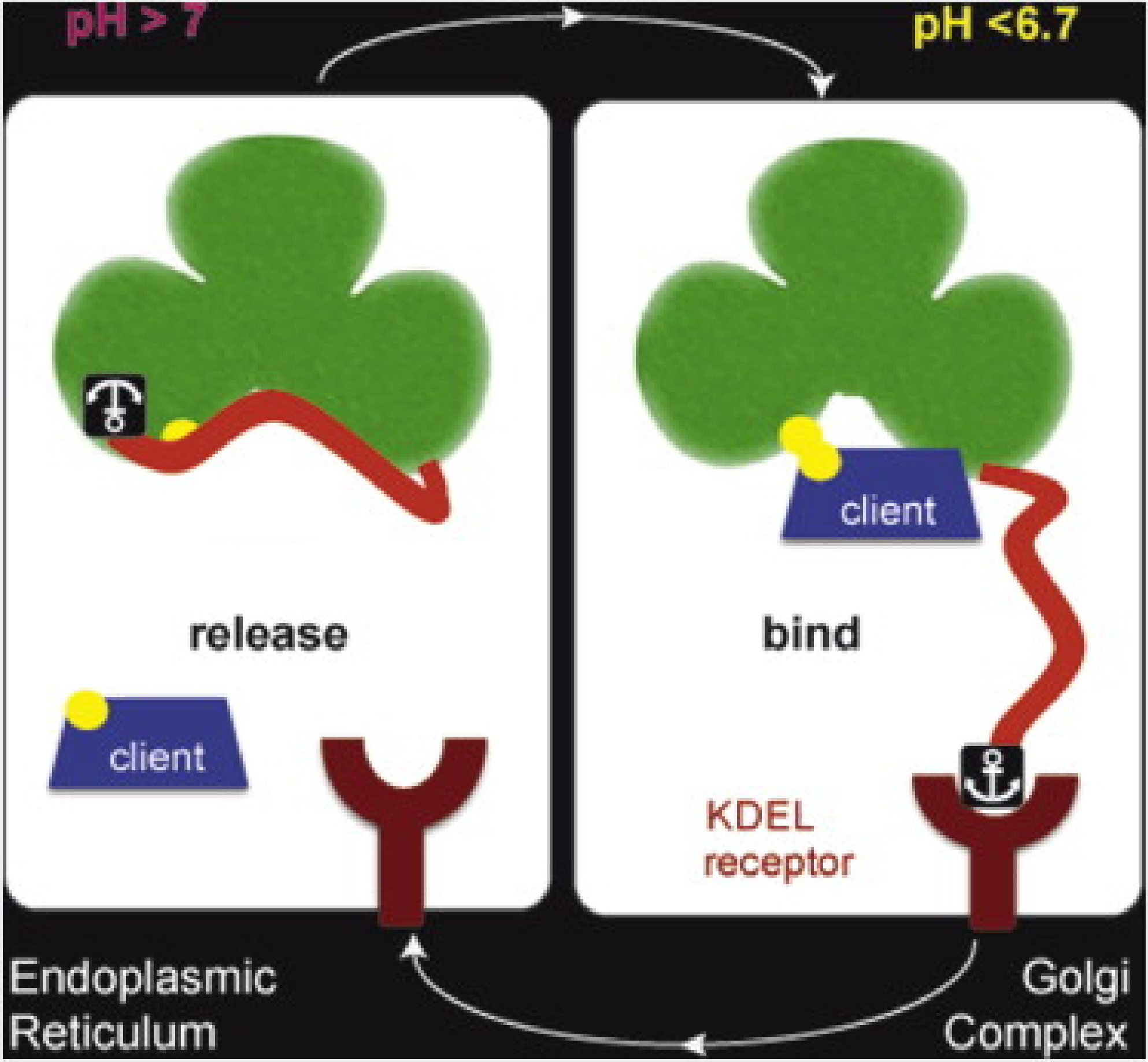
pH > 7
pH <6.7
release
client
bind
client
KDEL
receptor
Endoplasmic
Reticulum
Golgi
Complex

Molecular Cell
Article

A pH-Regulated Quality Control Cycle for Surveillance of Secretory Protein Assembly

Stefano Vavassori,[1,2,4,5] Margherita Cortini,[1,2,4,6] Shoji Masui,[3,4,7] Sara Sannino,[1,2,4] Tiziana Anelli,[1,2] Imma R. Caserta,[1] Claudio Fagioli,[1] Maria F. Mossuto,[1] Arianna Fornili,[1,8] Eelco van Anken,[1,2] Massimo Degano,[1] Kenji Inaba,[3,7] and Roberto Sitia[1,2,*]

[1]Divisions of Genetics and Cell Biology and Immunology, Transplantation and Infectious Diseases, San Raffaele Scientific Institute, 20132 Milan, Italy
[2]Università Vita-Salute San Raffaele, 20132 Milan, Italy
[3]Division of Protein Chemistry, Medical Institute of Bioregulation, Kyushu University, Fukuoka 812-8581, Japan
[4]These authors contributed equally to this work
[5]Present address: Département de Biochimie, Université de Lausanne, Epalinges CH-1015, Switzerland
[6]Present address: Department of Life Science, Università of Modena and Reggio Emilia, 42121 Modena, Italy
[7]Present address: Institute of Multidisciplinary Research for Advanced Materials, Tohoku University, Katahira 2-1-1, Aoba-ku, Sendai 980-8577, Japan
[8]Present address: Randall Division of Cell and Molecular Biophysics, King's College, New Hunt's House, London SE1 1UL, UK
*Correspondence: r.sitia@hsr.it
http://dx.doi.org/10.1016/j.molcel.2013.04.016

SUMMARY

To warrant the quality of the secretory proteome, stringent control systems operate at the endoplasmic reticulum (ER)-Golgi interface, preventing the release of nonnative products. Incompletely assembled oligomeric proteins that are deemed correctly folded must rely on additional quality control mechanisms dedicated to proper assembly. Here we unveil how ERp44 cycles between cisGolgi and ER in a pH-regulated manner, patrolling assembly of disulfide-linked oligomers such as IgM and adiponectin. At neutral, ER-equivalent pH, the ERp44 carboxy-terminal tail occludes the substrate-binding site. At the lower pH of the cisGolgi, conformational rearrangements of this peptide, likely involving protonation of ERp44's active cysteine, simultaneously unmask the substrate binding site and −RDEL motif, allowing capture of orphan secretory protein subunits and ER retrieval via KDEL receptors. The ERp44 assembly control cycle couples secretion fidelity and efficiency downstream of the calnexin/calreticulin and BiP-dependent quality control cycles.

INTRODUCTION

Protein folding in the endoplasmic reticulum (ER) is monitored by stringent quality control mechanisms that prevent release of immature or misfolded ER client proteins to travel further along the secretory pathway. Notable examples include the binding-and-release cycles of BiP, recognizing exposed hydrophobic stretches at the surface of nonnative conformers, and of calnexin/calreticulin, which exploit glucosylation status of N-linked glycans on ER client proteins to exert quality control (Ellgaard and Helenius, 2003). ER client proteins are rich in intra- and intermolecular disulfide bonds that are generally essential for their function. Numerous oxidoreductases reside in the ER to catalyze oxidative protein folding (Ellgaard and Ruddock, 2005). Also the process of disulfide bond formation is intimately linked to the quality control systems that prevent nonnative conformers to exit from the ER (Anelli and Sitia, 2008).

The same mechanisms that exert ER quality control on the folding of subunits also monitor certain steps in their oligomeric assembly. For instance, in the case of antibodies, BiP binds the first constant domain (CH1) of Ig heavy chain (H) and thereby retains it in the ER until it is displaced by the Ig light chain (L) to assemble into H_2L_2 structures, called "monomers" in the immunological jargon (Feige et al., 2009; Haas and Wabl, 1983; Hendershot and Sitia, 2005). The assembly process of μ_2L_2 monomers into IgM pentamers—$(\mu_2L_2)_5$J—and hexamers—$(\mu_2L_2)_6$—is favored by ERGIC-53 (Anelli et al., 2007), which resides preferentially in the ER-to-Golgi intermediate compartment (ERGIC) (Schindler et al., 1993).

Interaction of μ_2L_2 monomers with ERGIC-53 occurs upon release by BiP (Anelli et al., 2007), suggesting that these assemblies escape from the grasp of ER quality control and travel to more distal compartments of the early secretory pathway (Cortini and Sitia, 2010). This notion is perhaps not so surprising, as the μ_2L_2 monomers, even if not polymerized, are correctly folded and partially assembled and therefore no longer substrate to the ER chaperoning machinery. The only sign that betrays their unpolymerized state is the free tail-piece cysteine, which in mature IgM polymers is disulfide linked to corresponding cysteine residues in other μ_2L_2 monomers (Sitia et al., 1990). Members of the PDI family of oxidoreductases associate with free cysteines of orphan assembly subunits and thereby facilitate their so-called thiol-mediated retention (Fra et al., 1993; Reddy et al., 1996; Sitia et al., 1990).

We previously identified ERp44 as a PDI family member that covalently binds Ero1 oxidases and facilitates their intracellular localization (Anelli et al., 2002, 2003; Otsu et al., 2006). ERp44

is special for having a single cysteine (C29) in its conserved active site (CRFS), consistent with a dedicated role in thiol-mediated retention not only of Ero1 oxidases but also of orphan subunits of otherwise disulfide-linked oligomers, including IgM (Anelli et al., 2003, 2007) and adiponectin (Qiang et al., 2007; Wang et al., 2007). Moreover, ERp44 localizes predominantly to the ERGIC (Anelli et al., 2007; Gilchrist et al., 2006), unlike other PDI family members, which reside in the ER (Ellgaard and Ruddock, 2005). Still, the C-terminal −RDEL motif of ERp44 allows its capture by KDEL receptors (KDEL-R) in distal stations of the early secretory compartment, presumably for retrieval to the ER (Anelli et al., 2003). It is yet unclear how ERp44 cycles between its predominant localizations in the distal early secretory pathway and the ER, and how such cycling would relate to thiol-mediated retention.

Here we show that the pH gradient between cisGolgi and ER controls association of ERp44 both with its clients and with the KDEL-R. Our results suggest a model in which the simultaneous unmasking of the client and KDEL-R binding interfaces is facilitated by dislocation of the ERp44 C-terminal tail (C-tail), which in turn likely involves protonation state of the active site cysteine (C29) at cisGolgi-equivalent pH. As such, both ERp44 activity and its shuttling between the ER and cisGolgi are pH regulated to drive a quality control cycle dedicated to the surveillance of secretory protein assembly.

RESULTS

pH-Dependent Regulation of ERp44 Activity

ERp44 associates with its client proteins via disulfide linkages to residue C29 in the active site and noncovalent interactions with the surrounding hydrophobic patches at the substrate-binding site (Anelli et al., 2003; Wang et al., 2008). In the ERp44 crystal structure (Wang et al., 2008), however, the substrate binding site is shielded from the solvent by the C-tail that submerges into a groove delimited by the a and b′ domains (see also Figure 4A).

The pH gradient existing in the early secretory pathway (Figure 1A, top panel) regulates ERGIC-53 (Appenzeller-Herzog et al., 2004), a glycoprotein transporter lectin that shares several clients with ERp44, including IgM (Anelli et al., 2007). pH also regulates the in vitro binding of peptides to KDEL-R (Wilson et al., 1993), which prevent ERp44 secretion (Anelli et al., 2003). We thus surmised that the ERp44 structure, obtained from crystals grown at pH 7.5, most likely corresponds to an *off* conformation of the protein, found in the pH-neutral ER. Arrival into the distal, more acidic stations of the early secretory pathway, namely ERGIC and cisGolgi, could entail exposure of the substrate binding site (Figure 1A). We therefore assessed pH-dependent ERp44 C-tail rearrangements in vitro by 1-anilinonaphthalene-8-sulfonate (ANS) binding fluorescence spectroscopy (Serve et al., 2010). Consistent with the exposure of hydrophobic surfaces in ERp44, the ANS fluorescence peak was blue-shifted and enhanced when the pH was lowered from 7.5 to 6.5 (Figure 1B, top panel). This hypsochromic effect was largely abolished for a mutant in which we had engineered a disulfide bond between C29 and the C-tail (T369C, lower panel) to restrict its movements (Wang et al., 2008), unless the engineered disulfide bond was disrupted with the reducing agent DTT (Figure 1B). We concluded that accessibility of ERp44's substrate binding site involves pH-dependent dislocation of the C-tail.

Next, we monitored reactivity of the active site C29 as a function of pH and found that ERp44 bound more polyethylene glycol 2000-modified maleimide (MalPEG) as the pH was lowered from 8.0 to 6.0 (Figure 1C), with 50% MalPEG binding at pH 6.6 (Figure 1C, right panel, red dots). MalPEG binding faithfully reported on C29 reactivity, since its substitution with serine almost abolished binding. The residual binding observed in C29S involved residue C63 (Figure 1C, right panel, turquoise dots), as indicated by the absence of mobility shifts in the double mutant C29S-C63A (Figure 1C). Importantly, MalPEG binding to C29S was not influenced by pH. This finding excludes the possibility that the results obtained with ERp44 WT reflected pH dependence of MalPEG reactivity (Makmura et al., 2001). The T369C mutant did not bind MalPEG, reflecting the constitutive engagement of C29 in a disulfide bond with C369 (Figure 1C; Wang et al., 2008). Taken together, these results indicate that both C29 and the surrounding hydrophobic substrate binding site become more exposed at pH values similar to those encountered downstream of the ER.

C-Tail Rearrangements Determine Accessibility of the –RDEL ER Retrieval Motif

Although the −RDEL motif was not resolved in the crystal structure (Wang et al., 2008), we reasoned that its accessibility would be limited by the adjacent domain a when the C-tail is in a closed conformation, in turn hindering its availability to KDEL-R. Indeed, the "tail-locked" T369C mutant was secreted at levels comparable to a mutant lacking the −RDEL motif (ΔRDEL) (Figure 2, upper panels). Insertion of a spacer peptide (FLAG) immediately upstream of the RDEL tetrapeptide—to let it protrude from the protein—increased retention of the T369C mutant to levels similar to those for ERp44 WT with the FLAG insert (Figure 2 lower panels). The finding that FLAG-tagged ERp44 (whether WT or T369C mutant) was less well retained than "FLAG-less" ERp44 WT may reflect that RDEL recognition by KDEL-R depends in part on its context. Indeed, in ERp44 the sequence upstream of RDEL is remarkably conserved in metazoans (data not shown). In all, these data support the notion that an "open and flexible conformation" of the C-tail increases accessibility of the −RDEL retrieval motif to its cognate receptors.

ERp44 Retains Clients in the Early Secretory Compartment in a pH-Regulated Manner and Thereby Patrols Oligomeric Assembly of Disulfide-Linked Secretory Proteins

Having demonstrated in vitro that accessibility of the ERp44 active site is pH regulated, we set out to analyze pH dependency of ERp44 activity in vivo. To this end, we silenced expression of the Golgi pH regulator (GPHR) (Maeda et al., 2008), which specifically raised the pH in the cisGolgi by $\geq$0.4 units (Figure 3A). In line with our in vitro findings, neutralizing the ER-cisGolgi pH gradient inhibited ERp44 reactivity with its partners/substrates, as is evident from the GPHR silencing-induced decrease of ERp44 being engaged in disulfide-linked complexes (Figure 3B).

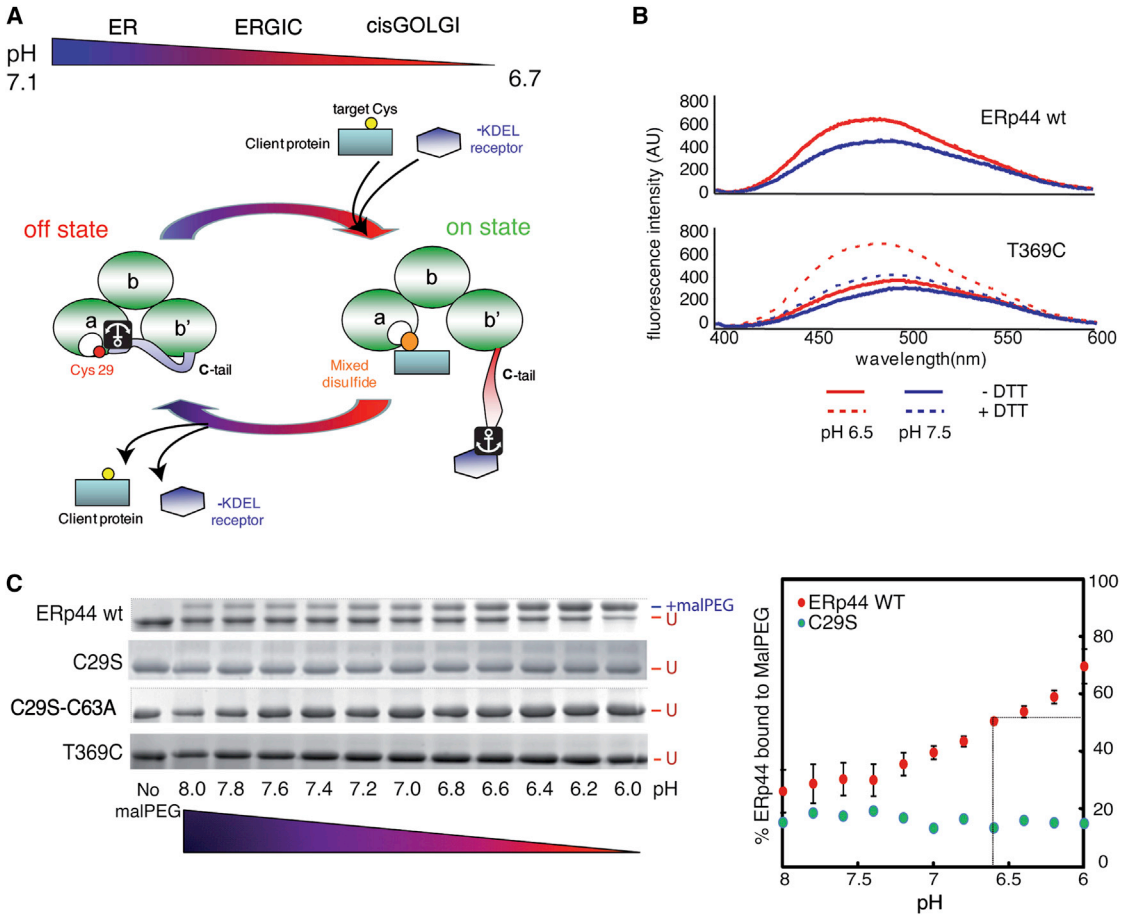

Figure 1. ERp44 Reactivity In Vitro Is pH Dependent

(A) Model for pH-dependent ERp44 quality control cycling. At neutral, ER-equivalent pH, ERp44 is mainly in an *off* conformation, corresponding to the structure resolved in crystals (Wang et al., 2008) with the C-tail closed. The lower pH in the cisGolgi provokes rearrangements of the C-tail that expose the substrate binding site (C29 in yellow and surrounding hydrophobic stretches in white) and −RDEL motif (depicted as an anchor), thus favoring client and KDEL-R binding, respectively. Capture by the KDEL-R engenders retrograde transport to the ER, where ERp44 may release both KDEL-R and client proteins to engage in further rounds of quality control, cycling through the early secretory pathway.

(B) pH-dependent conformational changes of ERp44. ANS fluorescence spectra were measured in the presence of recombinant ERp44 WT or the "tail-locked" T369C mutant in the presence or absence of DTT, at the indicated pH values. Exposure of hydrophobic surfaces correlates with increased and blue-shifted ANS fluorescence.

(C) pH-dependent accessibility of C29 in the substrate binding site. In vitro MalPEG binding causes reduced ERp44 gel mobility and was analyzed at various pH (U = unbound to MalPEG) to determine changes in the accessibility and reactivity of C29. The faint MalPEG-modified band in the C29S mutant is probably due to alkylation of C63, as it is absent in the C29S-C63A double mutant. Also the T369C mutant, in which C29 is bound covalently to C369 in the tail, did not bind MalPEG. At pH 6.6, about 50% of ERp44 WT is bound to MalPEG (see quantification on the right, red dots). Note that MalPEG binding C29S (tourquoise dots) does not change as a function of pH. Data are represented as average of three experiments ±SEM.

Consistently, thiol-mediated retention of ERp44 client proteins was inhibited upon GPHR silencing, as indicated by increased secretion of overexpressed Ero1α (Figures 3C and 3F and see Figure S2 online), adiponectin (APN, Figures 3C and 3F), and IgM assembly intermediates (Figures 3D and 3F).

Intracellular retention of Ero1α is a task that ERp44 shares with PDI, and overexpression of either ERp44 or PDI enhances Ero1α retention (Anelli et al., 2003; Otsu et al., 2006) (Figure 3C and Figure S2B). GPHR silencing strongly subdued this enhanced Ero1α retention when ERp44 was overexpressed, but much less so in the case of PDI overexpression (Figure 3C). Secretion of proteins that are not ERp44 clients, like α1-antitrypsin (α1AT) or a soluble GFP engineered for entry into the secretory pathway (sGFP), was also unaffected by raising the cisGolgi pH (Figures 3E and 3F). We concluded that ERp44-mediated retention in particular relies on the ER-cisGolgi pH gradient. Accordingly, retention of unassembled monomeric Ig-μ chains, which is mediated not by ERp44 but by the chaperone BiP, was pH insensitive (Figures 3D and 3F). Only when the CH1 domain, which is important for BiP binding (Haas and Wabl, 1983; Lee et al., 1999), is deleted (μΔCH1) or engaged in interactions with Ig-L chains (as in $\mu_2\lambda_2$ complexes) does ERp44 become the primary retainer of the Ig-μ chains, and hence their retention becomes pH dependent (Figures 3D and 3F).

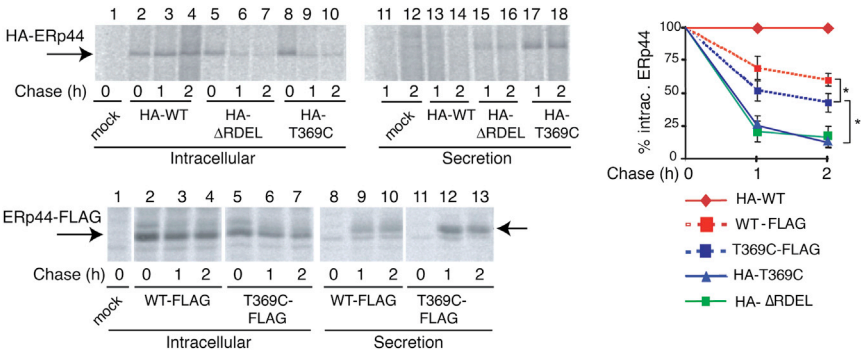

Figure 2. Rearrangements of the C-Tail Expose the –RDEL Motif

HeLa transfectants were pulsed with radiolabeled amino acids and chased in cold medium. At the indicated times, aliquots from the lysates (Intracellular) and supernatants (Secretion) were immunoprecipitated and analyzed by gel electrophoresis. Radiographs of a representative experiment are shown on the left; arrows indicate bands corresponding to overexpressed ERp44; the higher molecular weight of secreted ERp44 reflects posttranslational modifications (see also Anelli et al., 2003, 2007). Intracellular ERp44 levels were quantified from four to six experiments. Mean values and SEM are depicted in the graph shown on the right. Statistical significance was calculated by ANOVA one-way with Bonferroni's post test and indicated by brackets (T369C-FLAG-WT-FLAG, p = 0,041; T369C-T369C-FLAG, p = 0,006). In T369C, formation of a C29-C369 intrachain disulfide limits C-tail movements, likely impeding –RDEL binding to its receptors. Inserting a spacer peptide FLAG tag upstream –RDEL partially restores retrieval. The partial secretion of ERp44 WT upon insertion of a FLAG tag could depend on the acidity of the inserted peptide and/or its binding to the substrate binding site and hence reduced reactivity/accessibility of the –RDEL tetrapeptide.

Retention of sGFP-RDEL was pH insensitive (Figure 3E), as expected for a protein that lacks free cysteines and hence is not an ERp44 client. This finding implies at the same time that KDEL-R function, which is crucial for sGFP-RDEL retention, is not corrupted despite the rise in cisGolgi pH. Likewise, ERp44 was retrieved by KDEL-R despite GPHR silencing (Figure S2B), whereas this treatment allowed secretion of ERp44 client proteins (Figure 3F). Perhaps a partial C-tail opening in distal stations of the secretory pathway, which are less affected by GPHR silencing (Maeda et al., 2008), is sufficient for KDEL-R recognition but not for client binding.

The Reactive Site Cysteine 29 Is a Key Element in pH Regulation of C-Tail Opening and ERp44 Activity

Considering that the conformational changes that facilitate C-tail dislocation are induced by lowering the pH as ERp44 travels to the cisGolgi, we surmised that a protonation event may lie at the basis of the switch between the *on* and *off* conformations of ERp44. To explore this notion, we analyzed the crystal structure of ERp44 with the C-tail in the closed conformation using the program PROPKA3, a state-of-the-art semiempirical method that evaluates pKa values of ionizable residues starting from protein structures (Li et al., 2005; Olsson, 2011; Olsson et al., 2011). The most striking feature that emerged from the PROPKA3 analysis was the downward shift of the pKa of C29. Its predicted value of 7.7 units (Table 1) is significantly lower than the reference value for free cysteine in solution (9.0). This shift is mainly ascribed to the propensity of the neighboring side-chain hydroxyls of S32 and T369 and the main-chain amides of residues F31, S32, and T369 (Table 1 and Figure 4B) to form hydrogen bonds with C29 when in the thiolate form. Likewise, electrostatic interactions with the R98 side chain stabilize the thiolate form of C29 (Table 1). Based on this pKa value, a significant percentage of C29 would be in the thiolate form (41%) at pH 7.5 (Figure 4B and Table 1). Conversely, only 6.5% of C29 was predicted to be in the thiolate form at pH 6.5 (Table 1).

When we removed the β16 strand from the crystal structure in silico, simulating an "open" C-tail conformation of ERp44, the calculated pKa of C29 raised to 7.8 (Table 1). The effect was even more pronounced in sample structures at the end of molecular dynamics simulations of this Δβ16 model. As a consequence of a greater solvent exposure, loss of hydrogen bonding to T369, and an increased distance to the side chains of both S32 and R98, C29 had a calculated pKa of 8.7, implying that only a small percentage (6%) of C29 is in the thiolate form at pH 7.5 (Table 1 and Figure 4C).

Based on our in silico analyses, we mutated the residues predicted to affect the pKa of C29 in ERp44. Altering the side-chain groups such that they could no longer contribute to the stabilization of the thiolate form of C29 through hydrogen bonds or electrostatic interactions (S32A, R98Q, or T369A) indeed rendered ERp44 constitutively accessible to MalPEG and abolished the pH sensitivity of the reaction (Figure 4D). Deletion of strand β16 gave similar results (Figure 4D), supporting the notion that the S32A, R98Q, and T369A substitutions similarly led ERp44 to adopt the "open" C-tail conformation.

We then analyzed whether the enhanced accessibility of the ERp44 active site in the various mutants correlated with its affinity toward substrates. In surface plasmon resonance (SPR) assays (Masui et al., 2011), ERp44 WT showed a pH-dependent reactivity toward Ero1α, having a higher affinity for its partner at pH 6.5 than at pH 7.5 (Figure 4E). All the mutations that resulted in constitutive and pH-independent MalPEG binding of ERp44 made it also less pH dependent in SPR assays and increased its affinity for Ero1α (Figure 4E). The effect was weakest for the R98Q mutant, in agreement with the modest contribution of this arginine in stabilizing the thiolate form of C29 (Figure 4C).

In summary, our data indicate that C29, S32, R98, and T369 are components of the ERp44 pH-sensing mechanisms. The predicted pKa of C29 approaches neutral pH due to the interaction of its side chain with the surrounding residues, suggesting that its protonation, when ERp44 encounters the lower pH in the cisGolgi, is a key event for C-tail opening, and, hence, exposure of the substrate binding site.

pH Sensing by ERp44 In Vivo

We then further substantiated our findings on the mechanisms mediating ERp44 pH sensitivity by analyzing the phenotype of

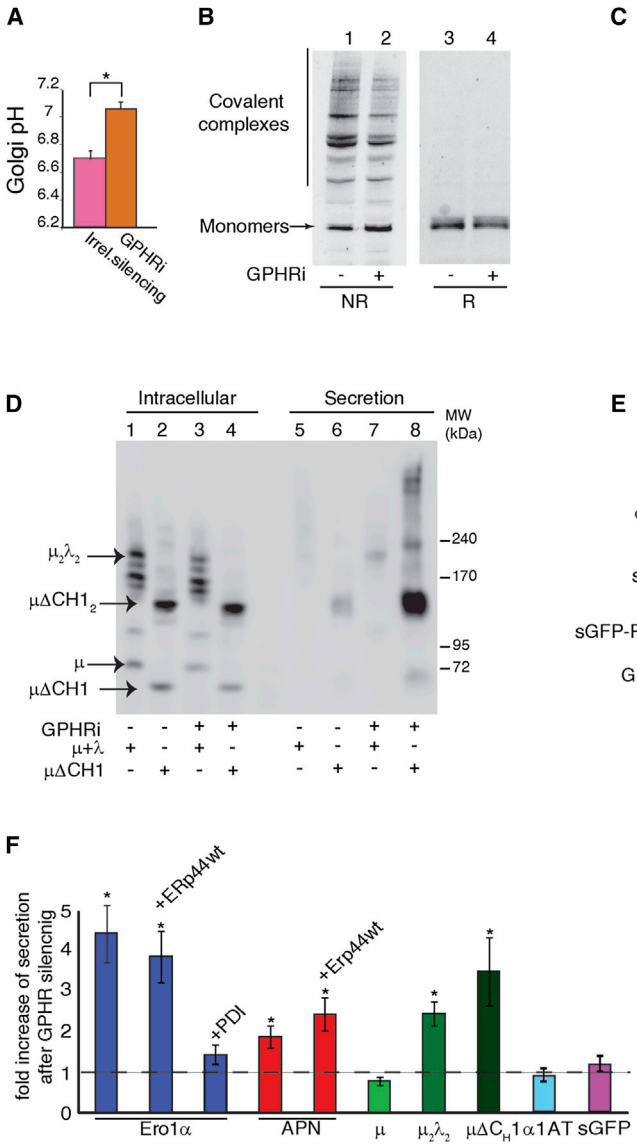

Figure 3. ERp44 Activity In Vivo Depends on the pH Gradient between ER and cisGolgi

(A) GPHR silencing ablates cisGolgi acidification. The pH in the cisGolgi was measured by organelle-targeted GPP130-pHluorins (Miesenböck et al., 1998), in HeLa cells expressing GPHR-specific or irrelevant siRNA, as indicated. Histograms display mean pH values ± SEM. *p = 0.001.

(B) GPHR silencing inhibits the accumulation of covalent complexes at steady state. Lysates of HeLa cells exposed to GPHR-specific (+) or irrelevant (–) siRNA were resolved under nonreducing (NR) or reducing (R) conditions in a 3%–8% acrylamide precasted gradient gel or in a 10% acrylamide gel, respectively. Nitrocellulose was decorated with monoclonal anti-ERp44 antibodies (36C9). As calculated by densitometric quantifications of two similar gels, the amount of ERp44 engaged in covalent complexes decreases by 40% after GPHRi.

(C and D) GPHR silencing specifically inhibits retention of ERp44 clients. Aliquots from lysates (Intracellular) and culture media (Secretion) were collected from HeLa transfectants expressing Ero1α (C, upper and lower panels), adiponectin (APN; C, midpanel), or Ig-μ, μΔCH1, Ig-λ (D), and subjected (+) or not (–) to GPHRi. ERp44 or PDI was coexpressed with Ero1α or adiponectin as indicated (C). (See also Figure S2.) Samples were analyzed under reducing or nonreducing conditions (C and D, respectively) and analyzed by immunoblotting with relevant antibodies. Bands corresponding to μ, μΔCH1, $\mu_2\lambda_2$, and $\mu\Delta CH1_2$ are indicated by arrows in (C).

(E) GPHR silencing does not affect transport of non-ERp44 clients, such as α1-AT or secretory green fluorescent protein extended a C-terminal RDEL peptide (sGFP-RDEL) or not (sGFP). Aliquots of cell lysates (Intracellular) and supernatants (Secretion) were collected and analyzed under reducing conditions.

(F) To compare the effects of GPHR silencing on the transport of the indicated proteins, the levels of intracellular and secreted proteins were quantified by densitometric analyses of four to ten experiments like the ones shown in (C)–(E) and Figure S2B. The percentage of secretion was then calculated relative to the intracellular pools. Histograms show the mean fold of induction upon GPHR silencing relative to cells treated with irrelevant siRNA ± SEM. Statistical significance was calculated using the paired Student's t test for parametric data. Ero1α, p = 0.038; Ero1α + ERp44 WT, p = 0.001; APN, p = 0.033; APN + ERp44 WT, p = 0.012; $\mu_2\lambda_2$, p = 0.004; μΔCH1, p = 0.040.

the above mutants in vivo. In line with the in vitro results, mutation of the residues expected to affect the pKa of C29 (S32, R98, and T369) dramatically increased the tendency of ERp44 to form covalent complexes with client and partner proteins, reaching levels comparable to a mutant lacking the whole β16 strand (see Figure 5A and Figure S3A). This was particularly evident when anti-HA antibodies were used to selectively analyze the behavior of the overexpressed transgenes (Figure S3A). We concluded that the S32A, R98Q, and T369A mutations increased the accessibility of C29 also in vivo, likely reflecting a more "open" conformation of the C-tail. In further support of our model, pH sensitivity of ERp44 activity was lost in all these mutants, since the fraction of molecules covalently bound to client and partner proteins did not decrease upon GPHR silencing in these mutants, as it did instead in ERp44 WT (Figure 5A). In addition, the activity of these mutants in retaining adiponectin was no longer sensitive to basification of the cisGolgi (Figure 5B and Figure S3B). Similar results were obtained also on Ero1α secretion (data not shown). Therefore, pH sensitivity is severely reduced when the critical residues S32, R98, and T369 are mutated and, consequently, the predicted C29 pKa is raised over neutral values.

DISCUSSION

The pH gradient between ER and Golgi may serve multiple roles in the cell, such as calibrating activity of lectins and Golgi

Table 1. Modulation of the pKa of C29 in ERp44 as Predicted by PROPKA3

		Percentage Thiolate at	Percentage Thiolate at		Side-Chain HB		Backbone HB			Coulombic			
Structure	pKa	pH 7.5	pH 6.5	Desolvation	S32	T369	F31	S32	T369	R30	R98	D64	K77
WT ERp44 Closed	7.66	40.9	6.5	2.09	−0.85	−0.85	−0.46	−0.83	−0.33	–	−0.12	0.01	–
Δβ16	7.84	31.4	4.4	1.06	−0.85	–	−0.46	−0.83	–	–	−0.09	–	–
Δβ16 MD Snapshot	8.7	5.9	0.6	0.71	−0.33	–	−0.04	−0.57	–	−0.03	−0.02	–	−0.02

Deconvolution of the contribution of C29 neighboring residues to the pKa shifts in ERp44. The pKa of residue C29 of the different ERp44 models was predicted using PROPKA3. The percentage of thiolate at a given pH was calculated using the equation $\%[\text{thiolate}] = K_A/([H^+]+K_A)$. The values reported in the Desolvation, Side-Chain HB, Backbone HB, and Coulombic columns are the pKa shifts from the model value in water (9.0) due to the different interactions listed. HB, hydrogen bond.

glycan-modifying enzymes (Paroutis et al., 2004). We have shown here that the pH gradient is exploited also for regulating quality control and secretion of a selection of key proteins. pH-regulated opening of ERp44's tail determines both client capture and KDEL-R-mediated retrieval. Thus, ERp44 governs a pH-regulated protein quality control cycle shuttling between cisGolgi, where ERp44 engages its clients, and the ER, where they must be released and where ERp44's C-tail presumably closes to occlude the client binding active site. Our in vitro MalPEG binding studies reveal a midpoint transition for ERp44 at a pH of approximately 6.6, a value similar to that found in the cisGolgi (Figure 3A). In all likelihood, however, additional mechanisms contribute to the regulation of ERp44 activity in living cells. For instance, interactions with KDEL-R may prevent closing of the C-tail and perhaps provide interaction with additional proteins.

Owing to the fact that the opening of the C-tail is pH dependent, the substrate binding site of ERp44 becomes more accessible progressively from ER to cisGolgi. Client proteins may thus engage ERp44 more proximally or distally along the early secretory pathway, according to their affinity toward the substrate binding site at a given pH. Differences in the pH optimum for ERp44 association may thus account for differences in the intracellular distribution of Ero1α, which is enriched at mitochondrial-associated ER membranes (Anelli et al., 2012; Simmen et al., 2010) and resides overall more distally in the early secretory pathway, as compared to another ERp44 client, SUMF1, which localizes to the more proximal stations (Fraldi et al., 2008).

In the crystal structure of ERp44, the active site C29 is buried at the interface between domain a and the C-tail (Wang et al., 2008). The environment in which C29 resides induces a downward pKa shift of this residue toward neutral values, de facto stabilizing the thiolate form of the amino acid. The negative charge of the deprotonated C29 restrains the C-tail movements via hydrogen bonds to S32 and T369 and electrostatic interactions with R98, which also interacts with the tail backbone. Upon entry of ERp44 into the cisGolgi compartment, C29 protonation likely occurs. This event, in turn, weakens C29 interactions with surrounding residues, as a cysteine with a side-chain thiol is less effective in forming the same hydrogen-bonding and long-range Coulombic interactions that the thiolate can maintain. How C29 of ERp44 reacts with clients to form mixed disulfides and whether ERp44 can act alone or requires assistance for this process deserves further investigation.

In line with our model, silencing of ERp44 causes more abundant secretion of many proteins with one or more exposed reactive cysteine, including Ig-μ (Anelli et al., 2007; Ronzoni et al., 2010), adiponectin (Wang et al., 2007; Qiang et al., 2007), SUMF1 (Fraldi et al., 2008; Mariappan et al., 2008), and peroxiredoxin 4 (T. Kakihana, K. Araki, S.V., I. Shun-ichiro, M.C., C.F., T. Natsume, R.S., and K. Nagata, unpublished data). Similarly, upon neutralization of the Golgi pH, ERp44 substrates like Ero1α, adiponectin, and IgM subunits are secreted more abundantly, presumably because the active site of ERp44 remains largely inaccessible. However, ERp44 itself is efficiently retained intracellularly. This observation suggests that ERp44 could partially open the C-tail, exposing its −RDEL, and interact with KDEL receptors without binding client proteins through an as-yet-unknown mechanism.

ERp44 receives substrates from, and associates with, ERGIC-53 (Anelli et al., 2007), a lectin that also embraces glycoproteins released by the calnexin/calreticulin quality control (Ellgaard and Helenius, 2003). The ERp44-ERGIC-53 tandem may thus integrate thiol-mediated and glycan-trimming-dependent ER quality control cycles. Similarly, we have shown that upon displacement by Ig-L, BiP no longer warrants retention of orphan Ig-H chains but leaves this role to ERp44 instead. ERp44 indeed is strongly upregulated in the course of B cell differentiation (van Anken et al., 2003; Anelli et al., 2007) to help avoid release of incompletely assembled IgM, which would jeopardize the efficiency of the humoral immune response. The ERp44 assembly control cycle thus embodies the last-resort quality control mechanism to prevent the untimely exit from the early secretory compartment of orphan subunits of otherwise disulfide-linked oligomeric secretory proteins.

EXPERIMENTAL PROCEDURES

Constructs

The cDNA encoding human ERp44 without the signal sequence was amplified by PCR and cloned into pET28 vector (from Novagen) at NheI and XhoI sites. The recombinant form of ERp44, which was overproduced in *E. coli*, lacks the −RDEL motif at the C terminus. Vectors for expression of HA-ERp44 in mammalian cells were previously described (Anelli et al., 2002). Mutants were obtained by polymerase chain reaction (PCR) or site-directed mutagenesis (SDM) (Table S1). Human ERp44-FLAG-RDEL was a kind gift of Professor K. Nagata (Kyoto-Sangyo University). The construct encoding the GPP130 pHluorin probe was a kind gift of Dr. J.E. Rothman (Center for High Throughput Cell Biology, Yale University). Plasmids encoding α1AT and adiponectin were kindly provided by Drs. R.N. Sifers (Baylor College of Medicine) and P. Scherer, respectively. pcDNA3.1-sGFP was obtained by appending the signal peptide

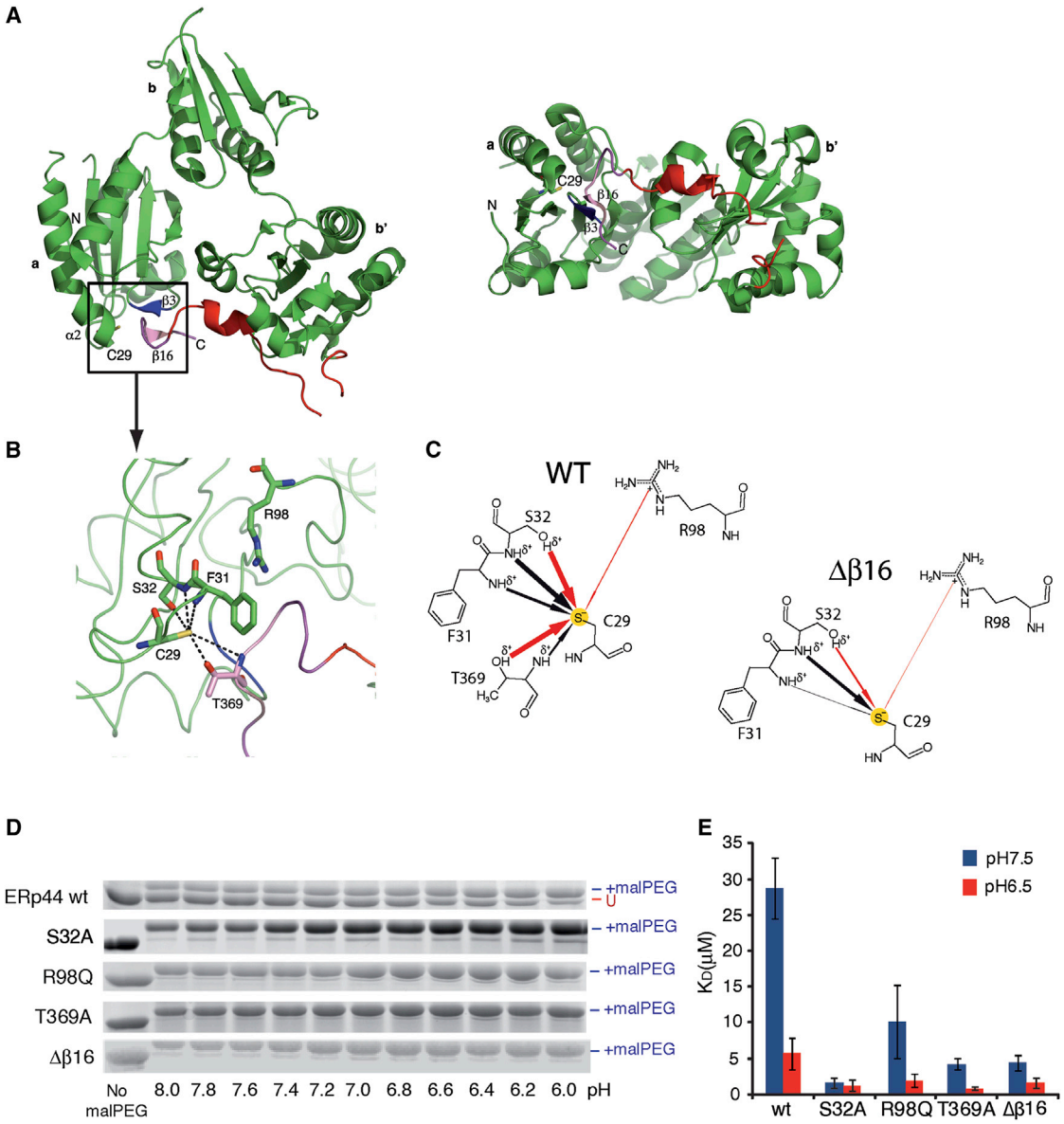

Figure 4. The Environment around C29 of ERp44 Modulates its pH-Dependent Reactivity at Physiological Values

(A) Overall structure of ERp44 (Wang et al., 2008), presented in two views related by a 90° rotation around the horizontal axis. The polypeptide folds into three thioredoxin-like domains (a, b, and b′); β strands are shown as arrows and α helices as ribbons. The C-terminal tail is colored in red, and strands β3 and β16 are colored blue and magenta, respectively. In the ERp44 crystal structure, residues of the β3 strand in domain a establish noncovalent interactions with the β16 strand in the C-tail, acting as a "molecular glue" that keeps the C-tail in the closed conformation.

(B) The panel shows a closer view of the active site C29, at the N-terminal portion of helix α2, highlighting interactions between C29 and neighboring residues shown as a stick models. Hydrogen bonds between polar atoms are shown as dashed lines. The positively charged guanidinium group in the side chain of residue R98 is 7.3 Å from the $S\gamma$ of C29.

(C) Two-dimensional diagrams showing the effect of the different interaction between C29 and amino acid residues on the thiol pKa in the crystal structure of ERp44 (top left panel) and in a representative snapshot from molecular dynamics simulations of the Δβ16 mutant (bottom right panel). The arrows represent interactions that decrease the pKa of C29, and their thickness is proportional to the magnitude of the reduction of C29 pKa by each residue shown (see also Table 1). The structural rearrangements following β16 removal greatly reduce the effect of the polar interactions on the thiol acidity. Red arrows indicate the interactions between side chains of each residue with C29 (which we could abolish through mutagenesis), while black arrows indicate interactions of C29 with the protein backbone.

(D) Increased accessibility of C29 in mutants with lower tendency to thiolate formation. The indicated mutants were reacted with MalPEG at different pH and resolved electrophoretically as described in Figure 1C. All the mutants show increased and pH-independent MalPEG reactivity.

(E) pH-dependent binding of ERp44to Ero1α. The K_D of association between recombinant Ero1α and WT or mutant ERp44 was determined by SPR at pH 6.5 and pH 7.5, as indicated. Histograms display the mean of at least four independent experiments ± SEM.

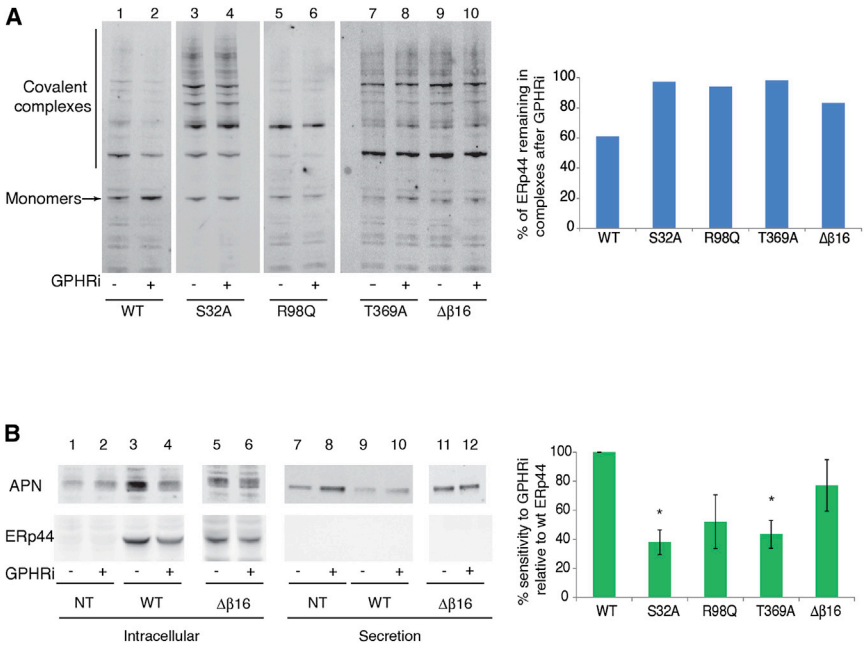

Figure 5. In Vivo Analysis of pH Sensor Mutants

(A) HeLa transfectants expressing the indicated ERp44 mutants were exposed to GPHR-specific (+) or irrelevant (−) oligonucleotides as described in Figure 3. Aliquots were resolved under nonreducing conditions and decorated with anti-ERp44 antibodies (36C9) that recognize also endogenous ERp44 (see also Figure S3A). Sensitivity to pH was calculated according to the formula (complexed ERp44/monomeric ERp44 under GPHRi) / (complexed ERp44/monomeric ERp44 under control conditions) * 100.

(B) HeLa transfectants expressing the indicated ERp44 mutants and adiponectin under GPHRi or control conditions were washed and cultured for 4 hr in fresh medium as also described in Figure S2. Aliquots of the lysates (Intracellular) and supernatants (Secretion) were resolved under reducing conditions and decorated with anti-adiponectin (APN) or anti-HA antibodies, which recognizes only transfected ERp44. One out of three independent experiments is shown for ERp44 WT and mutant Δβ16. Similar experiments were performed with other mutants (see also Figure S3). The graph shows the pH sensitivity of adiponectin retention [(secreted APN / intracellular APN under GPHRi) / (secreted APN / intracellular APN under control conditions) * 100 relative to the value obtained with ERp44 WT]. Data are represented as average of greater than or equal to three experiments ± SEM, and statistical significance was calculated using the Student's t test for parametric data. S32A, p = 0.041; T369A, p = 0.052.

of uromodulin to EGFP. Constructs were fully sequenced before utilization. Plasmids encoding WT and mutated secretory Ig-μ chains (μ_s and μΔCH1) were described in detail previously (Cenci et al., 2006; Mattioli et al., 2006).

Biochemical Techniques

The purification of wild-type and mutant ERp44 and Ero1α was performed as described (Inaba et al., 2010). The association and dissociation rate constants (k_{ON} or k_{OFF}) for the direct binding of ERp44 to immobilized Ero1α were determined by SPR measurements on a BIACORE2000 system (GE, Healthcare), in the presence of 1 mM GSH and 0.25 mM GSSG as described (Inaba et al., 2010). Experiments were replicated at least three times. Hyperactive Ero1α (with cysteines 104, 131, and 166 replaced by Ala) was used in SPR assays to limit variations caused by the autoregulatory mechanisms controlling Ero1α activity (Inaba et al., 2010). ANS fluorescence spectra were recorded in 1 cm cuvettes on a Hitachi F-4500 spectrofluorometer. ERp44 and mutants (5 μM) were mixed with 100 μM ANS in 20 mM Tris-HCl (pH 7.5) or MES (pH 6.5) containing 150 mM NaCl with or without 10 mM DTT and incubated at 293 K for 10 min.

Pulse-Chase, Immunoprecipitation, Western Blotting, and Densitometric Quantification

Cells were starved for 5 min in cysteine and methionine-free DMEM (GIBCO, Invitrogen), pulsed for 10 min with (^{35}S) cysteine and methionine (Easy Tag, Perkin-Elmer), washed twice, and chased for the indicated periods in complete medium. Cell lysates and supernatants were immunoprecipitated with anti-HA or anti-FLAG antibodies and resolved by SDS-PAGE. Fluorograms or western blot images were acquired with the Chemidoc-it Imaging System (UVP, Upland, CA) or with FLA-900 Starion (Fujifilm Life Science, USA) and quantified with Image Quant 5.2 as described (Anelli et al., 2007).

Cell Culture and Reagents

Tissue culture, transfection, and silencing were performed as described previously (Anelli et al., 2007). Fetal calf serum and cell culture medium were from GIBCO, Invitrogen. Unless otherwise indicated, chemicals were from Sigma. Polyclonal anti-mouse μ and anti-ERp44 (B68) antibodies were purchased from PRIMM srl (Milano, Italy). Rabbit polyclonal anti-adiponectin antibody was a kind gift of Dr. P. Scherer (University of Texas Southwestern Medical Center). Monoclonal anti-GFP (clones 7.1 and 13.1) was purchased from Roche (USA) and polyclonal anti-α1 antitrypsin (NCL A1Ap) from Novocastra. Monoclonal anti-ERp44 antibody (36C9) was previously described (Anelli et al., 2007). Goat anti-mouse μ and λ were from Southern Biotechnology Associates, Inc. Goat anti-mouse Ig and anti-rabbit Ig horse-radish peroxidase (HRP) were from Jackson ImmunoResearch Laboratories, Inc. Mouse monoclonal antibodies specific for Myc (9E10), HA (12CA5), and FLAG (M2) were immobilized by crosslinking to protein G and protein A beads, respectively. HRP rabbit anti-mouse IgG (H^+L) was from Dako Cytomation (Glostrup, CO).

Maleimidyl PEG-2K Modification of rERp44 Cys29

Each ERp44 derivative (5 μM) was incubated on ice for 30 min in various pH buffers containing 100 mM sodium phosphate and 150 mM NaCl, followed by incubation with maleimidyl PEG2K (300 μM) for 10 min at room temperature. The reaction was stopped by the addition of 5% trichloroacetic acid, and the protein pellet was washed with acetone and dissolved in buffer containing 50 mM Tris-HCl (pH 7.0) and 1% SDS before loading onto a reducing SDS gel (10%).

Measurement of Golgi pH by pHluorin Probes

HeLa cells expressing pME-Zeo-GPP130-pHluorin (Miesenböck et al., 1998) were cultured on glass-bottomed dishes and analyzed under a TCS SP2 Laser Scanning Confocal (Leica Confocal) equipped with an LD laser 405 (405 nm) and a multiline Ar laser (457, 488, and 515 nm) at room temperature. Data acquisition and analysis of intensity ratios (405 nm; 457 nm) were performed as described (Miesenböck et al., 1998). At least 120 regions of interest were analyzed by fluorescence microscopy. Statistical significance was calculated, comparing between conditions indicated by brackets using the two-tailed Student's t test.

RNAi

Oligonucleotides for RNA interference (Silencer Select predesigned siRNA products) were purchased from Ambion (siRNA ID #s56768). A final

concentration of 20 nM of each oligonucleotide was transfected. Lipofectamine RNAi MAX was from Invitrogen (Carlsbad, USA) and used for silencing in HeLa cells, according to the suppliers' instructions.

In Silico Calculations

We used the PROPKA 3.0 software (http://propka.ki.ku.dk) to predict the pKa value of ERp44 C29 and the role of surrounding amino acids starting from the crystal structure of the entire molecule (Wang et al., 2008; PDB ID code 2R2J) and from in silico models of the Δβ16 mutant. A description of the molecular dynamics simulations is presented in the Supplemental Information.

SUPPLEMENTAL INFORMATION

Supplemental Information includes three figures, one table, Supplemental Experimental Procedures, and Supplemental References and can be found with this article at http://dx.doi.org/10.1016/j.molcel.2013.04.016.

ACKNOWLEDGMENTS

We thank members of our labs for helpful suggestions, Jose Garcia-Manteiga and Alessandro Ambrosi for advice on statistical analyses, and the ALEMBIC Facility and Elena Pasqualetto for technical assistance. This work was supported by grants from Telethon (GGP11077), Associazione Italiana Ricerca Cancro (AIRC, IG10721, and 5 × 1000 SP9965), Fondazione Cariplo (NOBEL), Ministero della Salute, Regione Lombardia (ASTIL) to M.D. and R.S., and the Funding Program for Next Generation World-Leading Researchers from MEXT (to K.I.). S.M. is a research fellow of Japan Society for the Promotion of Science (JSPS). E.v.A. is supported through an Armenise Harvard Career Development Award and AIRC (MFAG13584 AIRC). M.F.M. is supported by a FEBS Fellowship. S.V., M.C., M.D., K.I., and R.S. designed the study and planned most of the experiments. S.V., S.M., and C.F. performed the in vitro experiments. M.C., S.S., T.A., and I.R.C. performed the in vivo experiments. A.F. and M.D. carried out the structural analysis and in silico studies. E.v.A., M.F.M., M.D., K.I., and R.S. helped in interpreting the results and with M.C. and S.V. played a major role in writing the manuscript.

Received: November 19, 2012
Revised: March 2, 2013
Accepted: April 10, 2013
Published: May 16, 2013

REFERENCES

Anelli, T., and Sitia, R. (2008). Protein quality control in the early secretory pathway. EMBO J. *27*, 315–327.

Anelli, T., Alessio, M., Mezghrani, A., Simmen, T., Talamo, F., Bachi, A., and Sitia, R. (2002). ERp44, a novel endoplasmic reticulum folding assistant of the thioredoxin family. EMBO J. *21*, 835–844.

Anelli, T., Alessio, M., Bachi, A., Bergamelli, L., Bertoli, G., Camerini, S., Mezghrani, A., Ruffato, E., Simmen, T., and Sitia, R. (2003). Thiol-mediated protein retention in the endoplasmic reticulum: the role of ERp44. EMBO J. *22*, 5015–5022.

Anelli, T., Ceppi, S., Bergamelli, L., Cortini, M., Masciarelli, S., Valetti, C., and Sitia, R. (2007). Sequential steps and checkpoints in the early exocytic compartment during secretory IgM biogenesis. EMBO J. *26*, 4177–4188.

Anelli, T., Bergamelli, L., Margittai, E., Rimessi, A., Fagioli, C., Malgaroli, A., Pinton, P., Ripamonti, M., Rizzuto, R., and Sitia, R. (2012). Ero1α regulates Ca(2+) fluxes at the endoplasmic reticulum-mitochondria interface (MAM). Antioxid. Redox Signal. *16*, 1077–1087.

Appenzeller-Herzog, C., Roche, A.C., Nufer, O., and Hauri, H.P. (2004). pH-induced conversion of the transport lectin ERGIC-53 triggers glycoprotein release. J. Biol. Chem. *279*, 12943–12950.

Cenci, S., Mezghrani, A., Cascio, P., Bianchi, G., Cerruti, F., Fra, A., Lelouard, H., Masciarelli, S., Mattioli, L., Oliva, L., et al. (2006). Progressively impaired proteasomal capacity during terminal plasma cell differentiation. EMBO J. *25*, 1104–1113.

Cortini, M., and Sitia, R. (2010). From antibodies to adiponectin: role of ERp44 in sizing and timing protein secretion. Diabetes Obes. Metab. *12*(*Suppl 2*), 39–47.

Ellgaard, L., and Helenius, A. (2003). Quality control in the endoplasmic reticulum. Nat. Rev. Mol. Cell Biol. *4*, 181–191.

Ellgaard, L., and Ruddock, L.W. (2005). The human protein disulphide isomerase family: substrate interactions and functional properties. EMBO Rep. *6*, 28–32.

Feige, M.J., Groscurth, S., Marcinowski, M., Shimizu, Y., Kessler, H., Hendershot, L.M., and Buchner, J. (2009). An unfolded CH1 domain controls the assembly and secretion of IgG antibodies. Mol. Cell *34*, 569–579.

Fra, A.M., Fagioli, C., Finazzi, D., Sitia, R., and Alberini, C.M. (1993). Quality control of ER synthesized proteins: an exposed thiol group as a three-way switch mediating assembly, retention and degradation. EMBO J. *12*, 4755–4761.

Fraldi, A., Zito, E., Annunziata, F., Lombardi, A., Cozzolino, M., Monti, M., Spampanato, C., Ballabio, A., Pucci, P., Sitia, R., and Cosma, M.P. (2008). Multistep, sequential control of the trafficking and function of the multiple sulfatase deficiency gene product, SUMF1 by PDI, ERGIC-53 and ERp44. Hum. Mol. Genet. *17*, 2610–2621.

Gilchrist, A., Au, C.E., Hiding, J., Bell, A.W., Fernandez-Rodriguez, J., Lesimple, S., Nagaya, H., Roy, L., Gosline, S.J., Hallett, M., et al. (2006). Quantitative proteomics analysis of the secretory pathway. Cell *127*, 1265–1281.

Haas, I.G., and Wabl, M. (1983). Immunoglobulin heavy chain binding protein. Nature *306*, 387–389.

Hendershot, L.M., and Sitia, R. (2005). Immunoglobulin assembly and secretion. In Molecular Biology of B Cells, T.A.F. Honjo and M.S. Neuberger, eds. (Amsterdam: Elsevier Acad Press), pp. 261–273.

Inaba, K., Masui, S., Iida, H., Vavassori, S., Sitia, R., and Suzuki, M. (2010). Crystal structures of human Ero1α reveal the mechanisms of regulated and targeted oxidation of PDI. EMBO J. *29*, 3330–3343.

Lee, Y.K., Brewer, J.W., Hellman, R., and Hendershot, L.M. (1999). BiP and immunoglobulin light chain cooperate to control the folding of heavy chain and ensure the fidelity of immunoglobulin assembly. Mol. Biol. Cell *10*, 2209–2219.

Li, H., Robertson, A.D., and Jensen, J.H. (2005). Very fast empirical prediction and rationalization of protein pKa values. Proteins *61*, 704–721.

Maeda, Y., Ide, T., Koike, M., Uchiyama, Y., and Kinoshita, T. (2008). GPHR is a novel anion channel critical for acidification and functions of the Golgi apparatus. Nat. Cell Biol. *10*, 1135–1145.

Makmura, L., Hamann, M., Areopagita, A., Furuta, S., Muñoz, A., and Momand, J. (2001). Development of a sensitive assay to detect reversibly oxidized protein cysteine sulfhydryl groups. Antioxid. Redox Signal. *3*, 1105–1118.

Mariappan, M., Radhakrishnan, K., Dierks, T., Schmidt, B., and von Figura, K. (2008). ERp44 mediates a thiol-independent retention of formylglycine-generating enzyme in the endoplasmic reticulum. J. Biol. Chem. *283*, 6375–6383.

Masui, S., Vavassori, S., Fagioli, C., Sitia, R., and Inaba, K. (2011). Molecular bases of cyclic and specific disulfide interchange between human ERO1alpha protein and protein-disulfide isomerase (PDI). J. Biol. Chem. *286*, 16261–16271.

Mattioli, L., Anelli, T., Fagioli, C., Tacchetti, C., Sitia, R., and Valetti, C. (2006). ER storage diseases: a role for ERGIC-53 in controlling the formation and shape of Russell bodies. J. Cell Sci. *119*, 2532–2541.

Miesenböck, G., De Angelis, D.A., and Rothman, J.E. (1998). Visualizing secretion and synaptic transmission with pH-sensitive green fluorescent proteins. Nature *394*, 192–195.

Olsson, M.H. (2011). Protein electrostatics and pKa blind predictions; contribution from empirical predictions of internal ionizable residues. Proteins *79*, 3333–3345.

Olsson, M.H., Chresten, R., Søndergaard, M., and Jensen, J.H. (2011). PROPKA3: consistent treatment of internal and surface residues in empirical pKa predictions. J. Chem. Theory Comput. *7*, 525–537.

Otsu, M., Bertoli, G., Fagioli, C., Guerini-Rocco, E., Nerini-Molteni, S., Ruffato, E., and Sitia, R. (2006). Dynamic retention of Ero1alpha and Ero1beta in the endoplasmic reticulum by interactions with PDI and ERp44. Antioxid. Redox Signal. *8*, 274–282.

Paroutis, P., Touret, N., and Grinstein, S. (2004). The pH of the secretory pathway: measurement, determinants, and regulation. Physiology (Bethesda) *19*, 207–215.

Qiang, L., Wang, H., and Farmer, S.R. (2007). Adiponectin secretion is regulated by SIRT1 and the endoplasmic reticulum oxidoreductase Ero1-L alpha. Mol. Cell. Biol. *27*, 4698–4707.

Reddy, P., Sparvoli, A., Fagioli, C., Fassina, G., and Sitia, R. (1996). Formation of reversible disulfide bonds with the protein matrix of the endoplasmic reticulum correlates with the retention of unassembled Ig light chains. EMBO J. *15*, 2077–2085.

Ronzoni, R., Anelli, T., Brunati, M., Cortini, M., Fagioli, C., and Sitia, R. (2010). Pathogenesis of ER storage disorders: modulating Russell body biogenesis by altering proximal and distal quality control. Traffic *11*, 947–957.

Schindler, R., Itin, C., Zerial, M., Lottspeich, F., and Hauri, H.P. (1993). ERGIC-53, a membrane protein of the ER-Golgi intermediate compartment, carries an ER retention motif. Eur. J. Cell Biol. *61*, 1–9.

Serve, O., Kamiya, Y., Maeno, A., Nakano, M., Murakami, C., Sasakawa, H., Yamaguchi, Y., Harada, T., Kurimoto, E., Yagi-Utsumi, M., et al. (2010). Redox-dependent domain rearrangement of protein disulfide isomerase coupled with exposure of its substrate-binding hydrophobic surface. J. Mol. Biol. *396*, 361–374.

Simmen, T., Lynes, E.M., Gesson, K., and Thomas, G. (2010). Oxidative protein folding in the endoplasmic reticulum: tight links to the mitochondria-associated membrane (MAM). Biochim. Biophys. Acta *1798*, 1465–1473.

Sitia, R., Neuberger, M., Alberini, C., Bet, P., Fra, A., Valetti, C., Williams, G., and Milstein, C. (1990). Developmental regulation of IgM secretion: the role of the carboxy-terminal cysteine. Cell *60*, 781–790.

van Anken, E., Romijn, E.P., Maggioni, C., Mezghrani, A., Sitia, R., Braakman, I., and Heck, A.J. (2003). Sequential waves of functionally related proteins are expressed when B cells prepare for antibody secretion. Immunity *18*, 243–253.

Wang, Z.V., Schraw, T.D., Kim, J.Y., Khan, T., Rajala, M.W., Follenzi, A., and Scherer, P.E. (2007). Secretion of the adipocyte-specific secretory protein adiponectin critically depends on thiol-mediated protein retention. Mol. Cell. Biol. *27*, 3716–3731.

Wang, L., Wang, L., Vavassori, S., Li, S., Ke, H., Anelli, T., Degano, M., Ronzoni, R., Sitia, R., Sun, F., and Wang, C.C. (2008). Crystal structure of human ERp44 shows a dynamic functional modulation by its carboxy-terminal tail. EMBO Rep. *9*, 642–647.

Wilson, D.W., Lewis, M.J., and Pelham, H.R. (1993). pH-dependent binding of KDEL to its receptor in vitro. J. Biol. Chem. *268*, 7465–7468.

Molecular Cell, Volume *50*

Supplemental Information

A pH-Regulated Quality Control Cycle for Surveillance of Secretory Protein Assembly

Stefano Vavassori, Margherita Cortini, Shoji Masui, Sara Sannino, Tiziana Anelli, Imma R. Caserta, Claudio Fagioli, Maria F. Mossuto, Arianna Fornili, Eelco van Anken, Massimo Degano, Kenji Inaba, and Roberto Sitia

Inventory of Supplemental Information

Supplemental Information provides 3 Supplemental Figures, 1 Supplemental Table, Supplemental Experimental Procedures, and Supplemental References; a brief description is given below.

- Supplemental Figure 1 (S1) provides a schematic representation of all ERp44 mutants used throughout the study.
- Supplemental Figure 2 (S2) shows a schematic representation of the transfection protocol used for the *in vivo* studies and an extended version of Figure 3B.
- Supplemental Figure 3 (S3) provides *in vivo* analysis of pH sensor mutants related to Figure 5. Non reducing gels for ERp44 mutants are shown in panel A while a comparative analysis of adiponectin secretion in the presence of the indicated mutants is shown in panel B.
- Supplemental Table 1 (S1) shows a list of all the primers employed throughout the study to generate ERp44 mutants.
- Supplemental Experimental Procedures provide details on the molecular dynamics simulation described in the main text in the paragraph entitled *"pH-regulation of C-tail opening accounts for ERp44 activity and involves protonation of the active site C29"*.
- Supplemental References are related to the Supplementary Experimental Procedures.

Supplemental Figures and Legends

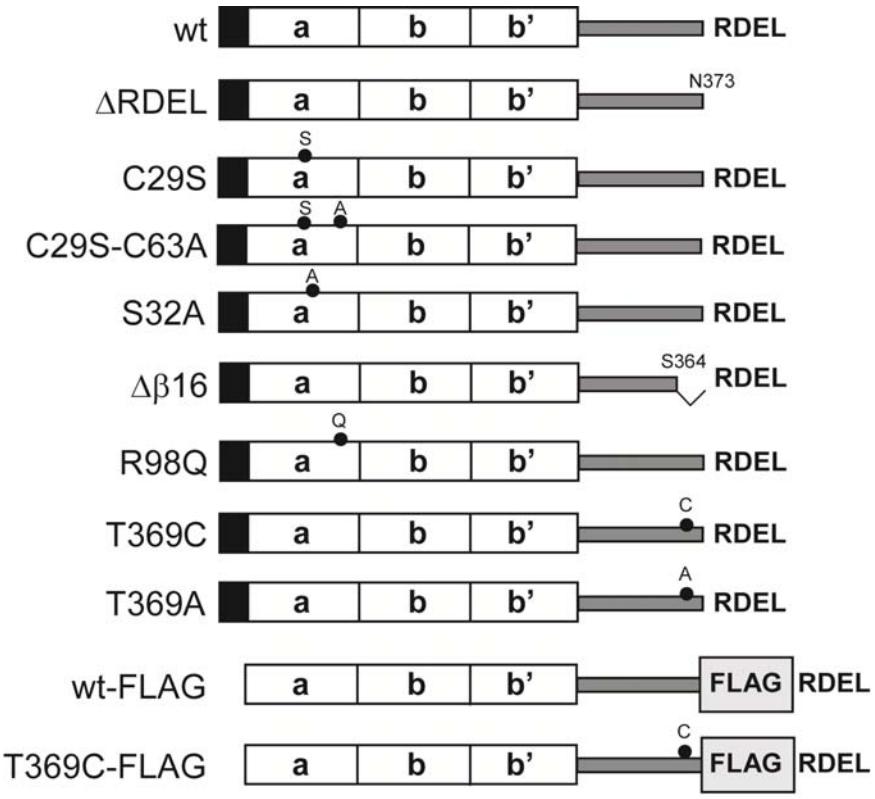

Supplemental Figure 1 (S1): Schematic representation of ERp44 mutants used in this study and related to all main text figures.

The three thioredoxin-like domains **a**, **b**, and **b'** are depicted as white rectangles. The C-tail is shown in grey. The FLAG is boxed in light grey. The C-terminal RDEL retention motif is indicated. The black square at N-terminus represents the HA tag, placed immediately downstream of the signal sequence. All constructs expressed in *E. coli* that were used in *in vitro* studies lack the tag, the N-terminal hydrophobic signal sequence and the C-terminal –RDEL motif. The latter is not resolved in the published crystal structure (PDB code: 2R2J, Wang et al., 2008) suggesting its high flexibility.

Black circles denote residues that were modified to the indicated residues by site directed mutagenesis. The coding sequence was severed at the indicated residues in deletion mutants (not in scale).

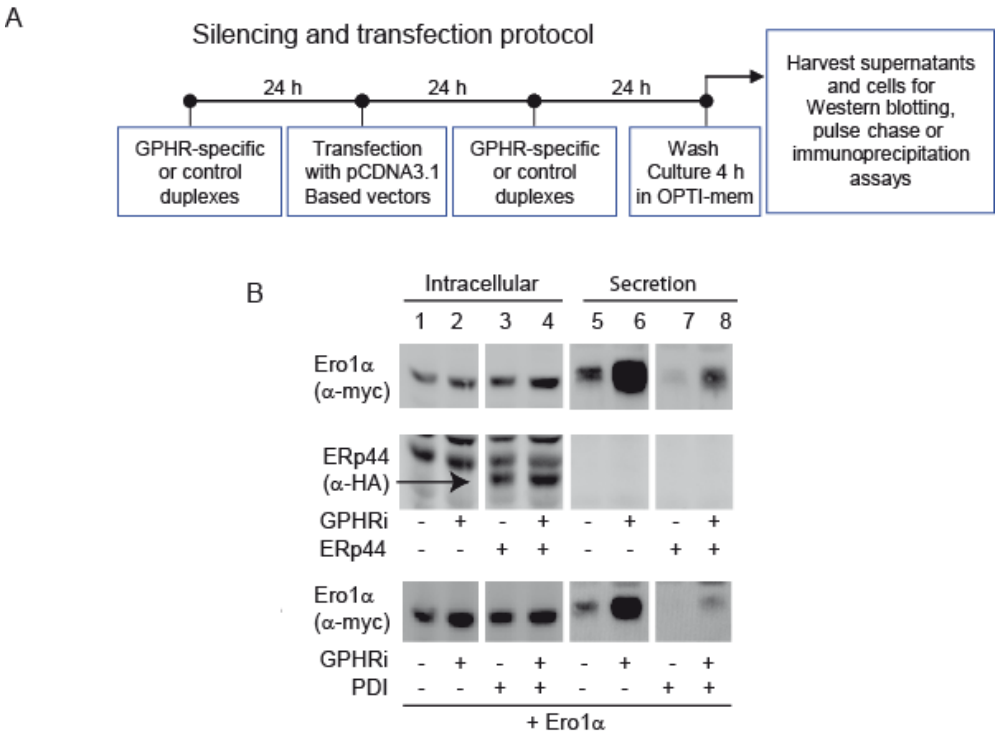

Supplemental Figure 2 (S2): The pH gradient along the early secretory compartment specifically regulates ERp44-mediated protein quality control (see also Figure 3).

A) Scheme of the transfection and silencing experiments shown in panel B and Fig. 3B-E. HeLa cells were silenced with specific or control oligonucleotides 72 and 24 h before analysis. Transfections were performed 48 h before analysis. Efficiency of GPHR silencing routinely exceeded 75%, as determined by mRNA quantification (not shown).

B) ERp44- but not PDI-mediated Ero1α retention is pH sensitive. HeLa transfectants expressing Ero1α alone or in conjunction with ERp44 or PDI were silenced with GPHR-specific or irrelevant siRNA. Lysates (Intracellular) and culture media (Secretion) were analyzed as in Fig. 3. The arrow points at over-expressed HA-tagged ERp44. Upper right panels for Ero1α secretion are identical to those in Fig. 3B. The slight increase in Ero1α secretion in PDI overexpressing cells (lane 8 of lower panel in part B of the Figure) likely reflects a residual role of ERp44 in Ero1α retention (Otsu et al., 2006).

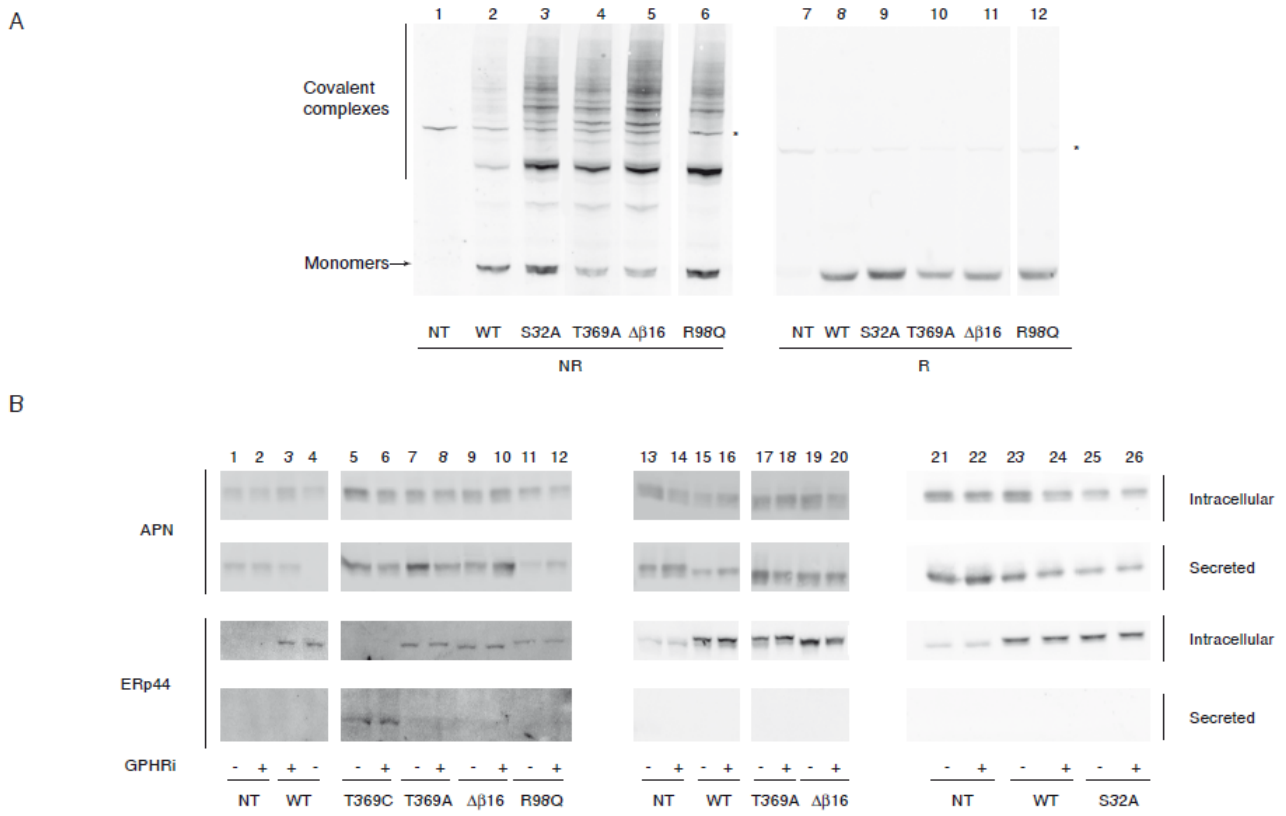

Supplemental Figure 3 (S3), related to figure 5: In vivo analysis of pH sensor mutants.

A) Aliquots of HeLa trasfectants expressing the indicated mutants were resolved under non reducing (NR) and reducing (R) conditions and decorated with anti HA antibody. Arrows indicate over-expressed monomeric ERp44. The * denotes a background band cross-reacting with our antibodies.

B) HeLa trasfectants expressing the indicated ERp44 mutants and adiponectin under GPHRi or control conditions were washed and cultured for 4 hours in fresh medium (see Fig. S2). Aliquots of the lysates (Intracellular) and culture media (Secretion) were resolved under reducing conditions and decorated with anti-adiponectin (APN), anti-HA or anti-ERp44 (36C9) antibodies, as indicated. Representative experiments are shown for different ERp44 mutants (S32A, R98Q, T369A, T369C, Δβ16).

Supplemental Experimental Procedures and Supplemental References

Molecular dynamics simulations

The X-ray structure of ERp44 (PDB code 2R2J) was used to prepare the starting configuration for molecular dynamics (MD) simulations. The Δβ16 structure was generated by deleting the coordinates of the Glu365-Arg372 segment. The missing loop in the **a** domain (Phe50-Glu53) was modelled with the ModLoop server (Fiser et al., 2000). The resulting structure was immersed in a cubic box (~ 97 x 97 x 97 $Å^3$) of ~ 29,000 TIP3P water molecules and 13 Na^+ counterions. Simulations and subsequent analyses were performed with GROMACS 3.3.3., using the ff-amber99sb porting (Sorin and Pande, 2005) of the AMBER parm99SB parameter set (Hornak et al., 2006). Periodic boundary conditions were imposed. The equations of motion were integrated using the leap-frog method with a 1-fs time step. The Berendsen algorithm was employed for temperature (T=300 K) and pressure (p=1 bar) regulation, with coupling constants of 0.1 ps. Bonds to hydrogen atoms were frozen with the LINCS method for the protein and the ligand, while SETTLE was used for water molecules. The Particle Mesh Method was used to calculate electrostatic interactions, with a 11-Å cutoff for the direct space sums, a 1.0-Å FFT grid spacing and a 6-order interpolation polynomial for the reciprocal space sums. For van der Waals interactions, a switching function was used with a double 9-10 Å cut-off. Long-range corrections to the dispersion energy were also included (Shirts et al., 2007). The system was first minimized with 2000 steps of steepest descent. Harmonic positional restraints (with a force constant of ~ 12 kcal/mol/ $Å^2$) were then imposed onto the protein heavy atoms and gradually turned off in 400 ps, while the temperature was increased from 200 to 300 K. The system was then simulated for 5 ns. To assess the reproducibility of the results, two trajectories were generated

for the wild type protein following the same protocol. The Δβ16 protein simulation was prolonged to 10 ns.

	Primers	Template	Plasmid		ERp44
Fw	GCACCCAGTGAATATAGGTATTGTCTATTGAGGGATTAACTCG	pET28 ERp44 wt	PET28	SDM	ERp44 T369C
Rv	CGAGTTAATCCCTCAATAGACAATACCTATATTCACTGGGTGC				
Fw	GTAAATTTTATGCTGACTGGGCTCGTTTCAGTCAGATGTTGC	pET28 ERp44 wt	PET28	SDM	ERp44C29A
Rv	GCAACATCTGACTGAAACGAGCCCAGTCAGCATAAAAATTTAC				
Fw	CACCCAGTGAATATAGGTATTGTCTATTGAGGGATCGAGATG	pCDNA ERp44 wt	pcDNA	SDM	ERp44T369C
Rv	CATCTCGATCCCTCAATAGACAATACCTATATTCACTGGGTG				
Fw	CCCAGCGAGTATAGGTATTGTTTATTGAGGGATCGAG	pEGFP N1	pEGFP N1	SDM	ERp44T369C Flag
Rv	CTCGATCCCTCAATAAACAATACCTATACTCGCTGGG	ERp44-Flag			
Fw	GTAAATTTTATGCTGACTGGGCTCGTTTCAGTCAGATGTTGC	pCDNA ERp44 wt	pcDNA	SDM	ERp44C29A
Rv	GCAACATCTGACTGAAACGAGCCCAGTCAGCATAAAAATTTAC				
Fw	CCTTCCAGAAACTAGCACCCAGTTAATATAGGTATACTCTATTGAGG	pCDNA ERp44 wt	pcDNA	SDM	ERp44Δβ16
Rv	CCTCAATAGAGTATACCTATATTAACTGGGTGCTAGTTTCTGGAAGG				
Fw	CAACTCGAGCGTTACCATGCATCCTGCC	pCDNA ERp44 wt	pcDNA	PCR	ERp44Δβ16
Rv	GCGCGGTACCTTAAAGCTCATCTCGACTGGGTGCTAGTTTCTGGAAG			cloning	
Fw	GAGAATACAGGGGTCAGCAGTCAGTGAAAGCATTGGC	pET28 ERp44 wt	PET28	SDM	ERp44R98Q
Rv	GCCAATGCTTTCACTGACTGCTGACCCCTGTATTCTC				
Fw	GAGAATACAGGGGTCAGCAGTCAGTGAAAGCATTGGC	pCDNA ERp44 wt	pcDNA	SDM	ERp44R98Q
Rv	GCCAATGCTTTCACTGACTGCTGACCCCTGTATTCTC				
Fw	GAAACTAGCACCCAGTGAATATCAGTATACTCTATTGAGGGATCG	pCDNA ERp44 wt	pcDNA	SDM	ERp44R367Q
Rv	CGATCCCTCAATAGAGTATACTGATATTCACTGGGTGCTAGTTTC				
Fw	GCACCCAGTGAATATCAGTATACTCTATTGAGG	pET28 ERp44 wt	PET28	SDM	ERp44R367Q
Rv	CCTCAATAGAGTATACTGATATTCACTGGGTGC				
Fw	TTTGCCAGAGTTGATGCCGATCAGCACTCTGAC	pET28 ERp44	PET28	SDM	ERp44C29A
Rv	GTCAGAGTGCTGATCGGCATCAACTCTGGCAAA	C29A			C63A
Fw	GCTGACTGGTGTCGTTTCGCTCAGATGTTGCATCCAATT	pCDNA ERp44 wt	pcDNA	SDM	ERp44S32A
Rv	AATTGGATGCAACATCTGAGCGAAACGACACCAGTCAGC				

Supplemental Table S1: List of the primers and methods (SDM, side directed mutagenesis; PCR, polymerase chain reaction) employed to generate ERp44 mutants used in all main text figures.

Supplemental References

Fiser, A., Do, R.K., and Sali, A. (2000). Modeling of loops in protein structures. Protein Sci *9*, 1753-1773.

Hornak, V., Abel, R., Okur, A., Strockbine, B., Roitberg, A., and Simmerling, C. (2006). Comparison of multiple Amber force fields and development of improved protein backbone parameters. Proteins *65*, 712-725.

Shirts, M.R., Mobley, D.L., Chodera, J.D., and Pande, V.S. (2007). Accurate and efficient corrections for missing dispersion interactions in molecular simulations. J Phys Chem B *111*, 13052-13063.

Sorin, E.J., and Pande, V.S. (2005). Empirical force-field assessment: The interplay between backbone torsions and noncovalent term scaling. J Comput Chem *26*, 682-690.

Molecular Cell
Previews

Acidification Activates ERp44—A Molecular Litmus Test for Protein Assembly

Linda M. Hendershot,[1,*] Matthias J. Feige,[1,*] and Johannes Buchner[2,*]
[1]Department of Tumor Cell Biology, St. Jude Children's Research Hospital, 262 Danny Thomas Place, Memphis, TN 38105, USA
[2]Center of Integrated Protein Science at the Department Chemie of the Technische Universität München, Lichtenbergstrasse 4, 85748 Garching, Germany
*Correspondence: linda.hendershot@stjude.org (L.M.H.), matthias.feige@stjude.org (M.J.F.), johannes.buchner@tum.de (J.B.)
http://dx.doi.org/10.1016/j.molcel.2013.06.008

In this issue of *Molecular Cell*, Vavassori et al. (2013) show that a pH-induced conformational change in the quality control protein ERp44 allows retrieval of secretory proteins that contain free thiols via a disulfide linkage from postendoplasmic reticulum compartments to prevent their premature secretion.

One-third of the mammalian genome encodes proteins that either populate the secretory pathway or travel through it on to their final destinations at the cell surface or the extracellular milieu. Proteins destined for secretion are folded and assembled in the endoplasmic reticulum (ER) before they proceed through the Golgi en route to the cell surface. As cellular communication and the organism's homeostasis depend on the fidelity of secreted and transmembrane proteins, the ER is equipped with a machinery of folding helpers that also scrutinizes the outcomes of these processes. In many cases, folding involves the assembly of multiple subunits that are stabilized by intermolecular disulfide bonds. Unassembled subunits with free cysteines are recognized and retained in the cell by the PDI family member ERp44 via covalent linkages. Key steps in the regulation of this process are unveiled in a paper by Vavassori et al. in this issue of *Molecular Cell* (Vavassori et al., 2013).

An early model for transport in the secretory pathway was that proteins generally moved forward ("bulk flow") unless they were specifically retained. Significant support was given to this idea when many of the soluble ER-resident proteins, such as ER chaperones and oxidoreductases that interact directly with nascent proteins, were shown to possess the tetrapeptide sequence KDEL at their C terminus, which was recognized by the KDEL receptor present in the intermediate compartment between the ER and the *cis*-Golgi (ERGIC) (Munro and Pelham, 1987). KDEL-containing components of the ER quality control machinery and their bound cargo are returned to the ER upon engaging this receptor (Wilson et al., 1993). This prevents the escape of subunits of multimeric complexes that must assemble to complete their folding like immunoglobulin heavy chains. Unassembled Ig subunits are promptly returned to the ER via their association with the chaperone BiP, which recognizes their unfolded regions (Lee et al., 1999; Feige et al., 2009). Further features of incompletely folded or oxidized proteins are monitored by PDI family members and the lectin chaperone system of the ER (Braakman and Bulleid, 2011; Bulleid and Ellgaard, 2011).

While concepts for the assistance and surveillance of folding and oxidation by molecular chaperones and oxido-reductases are well established, the post-chaperone stage that oversees correct oxidative assembly of proteins that have otherwise completed folding is less well understood, in terms of both mechanisms and subcellular locations. IgM and IgA heavy chains, for example, require additional disulfide links with a protein called J chain to form pentamers and dimers, respectively. Unlinked C-terminal cysteines present on these heavy chains are recognized by ER PDI family members, including ERp44, in a process known as "thiol-mediated retention" (Anelli et al., 2003; Sitia et al., 1990).

Although the retrieval of these substrates utilizes the KDEL receptor system, unlike most ER chaperones and oxidases, ERp44 binds to client proteins in the ERGIC or *cis*-Golgi subcompartments, instead of the ER, where it forms a covalent complex via its single active site cysteine, Cys29 (Anelli et al., 2003). The crystal structure of ERp44, however, revealed that the C-terminal tail of the protein covers both its putative hydrophobic substrate binding site and Cys29 (Figure 1A) and appeared to shield the ER retention sequence (Wang et al., 2008), raising further questions about this unusual chaperone. Sitia and coworkers speculated that this structure might represent an inactive ER conformation, as the crystals were grown at pH 7.5 (Wang et al., 2008), which is similar to the pH of the ER, and proposed that the slightly more acidic ERGIC/*cis*-Golgi compartments might trigger a conformational change that both unleashes the active site and switches ERp44 to a recycling mode. Consistent with this possibility, Vavassori et al. (2013) report that hydrophobic sites and Cys29 become increasingly accessible in vitro as pH decreases, whereas covalently fixing the C-terminal tail (including the RDEL motif) to the active site Cys29 inhibited both pH-dependent changes (Figure 1A). The authors hypothesized that protonation of Cys29 itself underlies the pH-dependent conformational changes of ERp44. Based on this idea, they created ERp44 mutants that were predicted to raise the pKa of Cys29, and indeed these ERp44 mutants had increased affinity for substrate proteins,

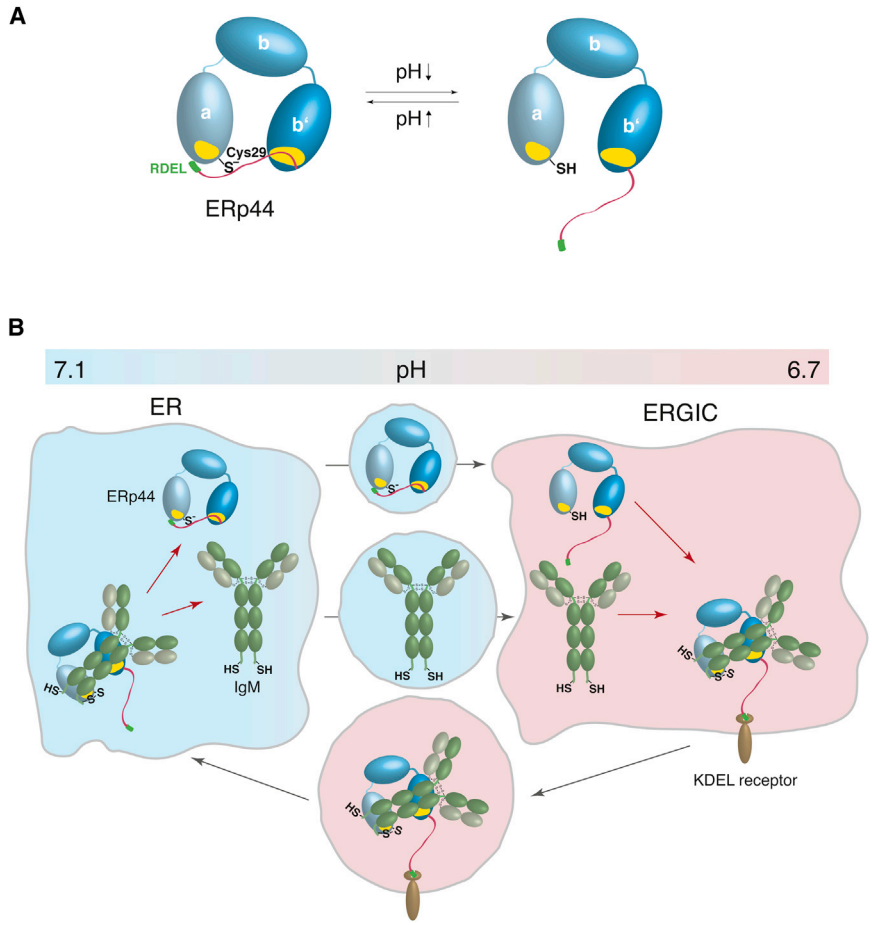

Figure 1. A Model for the pH-Mediated Conformational Changes in ERp44 Regulating Its Activity In Vivo

(A) ERp44 consists of three thioredoxin-like domains (a, b, and b′) and a C-terminal tail (shown in red) that contains the ER-retention motif RDEL (shown in green). Upon lowering the pH, Cys29 becomes protonated, leading to a conformational change that simultaneously exposes a hydrophobic site in domain b′ (hydrophobic sites in domain a and b′ are shown in yellow), the reactive Cys29, and the RDEL motif.

(B) ERp44 and its substrates (e.g., an IgM monomer) leave the ER independently for the ERGIC. There, the lower pH activates ERp44 (see A), allowing formation of a covalent ERp44-substrate disulfide bond and exposure of the RDEL motif. This links the incompletely assembled protein subunit: chaperone complex to the KDEL ER-retention system, providing a mechanism to return the substrate to the ER for further assembly or degradation. Red arrows indicate steps that are not yet resolved mechanistically.

which was no longer influenced by pH changes. The combination of in vitro and in silico data provides an appealing explanation for ERp44's activation.

Complimentary studies were performed to test for the pH-regulated conformational switch in ERp44 in vivo by reducing the expression of the Golgi pH regulator, GPHR, which interferes with acidification of the Golgi (Maeda et al., 2008). This significantly reduced the retention of IgM subunits as well as two other ERp44 substrates, adiponectin and Ero1α. Interestingly, basification of the Golgi did not affect the retention of RDEL-tagged GFP, arguing that the pH-induced changes in ERp44, as opposed to effects on the KDEL receptor interaction, underlie the observed phenomena. The mutants that rendered ERp44 constitutively active in vitro were also no longer affected by pH changes in vivo, arguing that a similar mechanism was at play. However, the different patterns of mutant activities observed suggest additional complexity in cells that might represent other unanticipated effects on the active species of ERp44 and/or substrate release in the ER.

The picture emerging from this study (Figure 1B) is that the slightly alkaline pH of the ER inactivates ERp44, whereas the more acidic compartments along the secretory pathway induce an activating conformational switch in ERp44. This separates the activities of the folding and redox machinery in the ER from the ERp44-mediated quality control in both time and space, and provides a new perspective on thiol-mediated retention. Thus, unassembled protein subunits or proteins that rely on ERp44 for ER retention will be efficiently detected soon after leaving the ER by the now-activated ERp44 and transported back to the ER.

However, it remains unclear exactly how the covalent linkage of ERp44 with its substrates is formed, as disulfide bonds within the active site of PDIs are transferred to induce oxidative folding and assembly of substrates (Bulleid and Ellgaard, 2011). Perhaps covalent dimers of ERp44 linked via Cys29 represent the active species, providing a disulfide bond that could be attacked by substrate thiol groups. Dimerization of ERp44 could be influenced by the various mutations, suggesting an explanation for the differences observed. Also, the fate of the ERp44-substrate complex once it returns to the ER remains unknown. It is possible that it is reduced by an ER-resident oxido-reductase allowing the cycle to continue, or alternatively the ER quality control machinery might end the cycle and target the substrate for degradation. The study by Sitia and coworkers (Vavassori et al., 2013) sets the stage to address these interesting questions.

REFERENCES

Anelli, T., Alessio, M., Bachi, A., Bergamelli, L., Bertoli, G., Camerini, S., Mezghrani, A., Ruffato, E., Simmen, T., and Sitia, R. (2003). EMBO J. *22*, 5015–5022.

Braakman, I., and Bulleid, N.J. (2011). Annu. Rev. Biochem. *80*, 71–99.

Bulleid, N.J., and Ellgaard, L. (2011). Trends Biochem. Sci. *36*, 485–492.

Feige, M.J., Groscurth, S., Marcinowski, M., Shimizu, Y., Kessler, H., Hendershot, L.M., and Buchner, J. (2009). Mol. Cell *34*, 569–579.

Lee, Y.K., Brewer, J.W., Hellman, R., and Hendershot, L.M. (1999). Mol. Biol. Cell *10*, 2209–2219.

Maeda, Y., Ide, T., Koike, M., Uchiyama, Y., and Kinoshita, T. (2008). Nat. Cell Biol. *10*, 1135–1145.

Munro, S., and Pelham, H.R. (1987). Cell *48*, 899–907.

Sitia, R., Neuberger, M., Alberini, C., Bet, P., Fra, A., Valetti, C., Williams, G., and Milstein, C. (1990). Cell *60*, 781–790.

Vavassori, S., Cortini, M., Masui, S., Sannino, S., Anelli, T., Caserta, I.R., Fagioli, C., Mossuto, M.F., Fornili, A., van Anken, E., et al. (2013). Mol. Cell *50*, this issue, 783–792.

Wang, L., Wang, L., Vavassori, S., Li, S., Ke, H., Anelli, T., Degano, M., Ronzoni, R., Sitia, R., Sun, F., and Wang, C.C. (2008). EMBO Rep. *9*, 642–647.

Wilson, D.W., Lewis, M.J., and Pelham, H.R. (1993). J. Biol. Chem. *268*, 7465–7468.

p53: The TRiC Is Knowing When to Fold 'Em

Jessica Monteith[1] and Steven B. McMahon[1,*]
[1]Department of Cancer Biology, Thomas Jefferson University, Philadelphia, PA 19107, USA
*Correspondence: steven.mcmahon@jefferson.edu
http://dx.doi.org/10.1016/j.molcel.2013.06.009

In this issue, Trinidad et al. (2013) show that CCT/TRiC is a chaperone required for p53 folding, thus providing another layer of regulation of p53 function, with implications for cancer therapeutics targeting the p53 pathway.

Loss of p53 function in human cancer most frequently occurs via single amino acid missense mutations (Edlund et al., 2012). Missense mutations that destroy the normal function of p53 are only part of the story, however; many of these p53 mutants do not only lose normal function but also gain functions that enhance tumor progression (Halevy et al., 1990). Among the new functions acquired by mutant p53, the best-characterized is the ability to drive the invasive growth of tumor cells (Muller et al., 2009). It is in this chapter of the story that the results of Trinidad et al. (2013; in this issue of *Molecular Cell*) provide an unexpected twist. They show that the ability to enhance invasive growth is not strictly a property of mutant forms of p53 but is conferred even by the wild-type p53 protein if its proper folding is blocked.

Specifically, in a search for new partners that might selectively bind mutant p53 and explain its gain-of-function activities, Trinidad et al. (2013) made the somewhat remarkable discovery that seven of the eight proteins that comprise the CCT chaperone complex interact with both mutant and wild-type p53. CCT (or TRiC) is an evolutionarily conserved, 16 subunit complex that contains two copies of each of the eight individual proteins (i.e., a dimer of identical octamers) (Yébenes et al., 2011). The central function of CCT is to mechanically enforce the correct folding of its client proteins, via a process that requires ATP hydrolysis.

So what role might this professional protein-folding complex be playing in controlling the structure of p53? And why is it interacting with both the wild-type protein and a mutant whose structure is so corrupted that it no longer functions to suppress cancer? To help us understand the issues, we have two decades of increasingly elegant structural studies of p53 to guide us (reviewed in Okorokov and Orlova, 2009). p53 is an obligate and intricate homotetramer that also interacts in a nucleotide sequence-specific manner with its palindromic binding sites in the genome. One of the major classes of p53 mutations in human cancer inactivates the protein by altering the conformation of the tetramer; a second blocks its interaction with the DNA binding site, without inducing overt structural defects.

Understanding chaperones like CCT that regulate the folding of p53 has important clinical implications. Clever strategies have begun to emerge that use small molecules or peptides (e.g., PRIMA-1met) to correct misfolded mutant p53 protein in tumor cells, thus allowing the protein to regain some of the biochemical activities that are required for tumor suppression (Issaeva et al., 2003). In addition to genetic lesions in p53 itself, human cancer cells have discovered other creative ways to inactivate this critical tumor suppressor, including overexpression of p53 inhibitors like MDM2 and loss of p53 activators like p14ARF/CDKN2A (Levine and Oren, 2009). The discoveries of Trinidad et al. (2013) suggest that inactivation of CCT function could be a very efficient mechanism by which a tumor cell might deactivate the tumor-suppressor function of p53 and simultaneously enhance its gain-of-function activities that are protumorigenic. Is there any evidence for this? In fact there is modest yet rapidly accumulating evidence that CCT is altered in cancer, and public repositories like COSMIC show mutations in several of the CCT subunits (Forbes et al., 2011). Whether these mutations activate or inactivate CCT (or are inert) remains to be determined, but this newly discovered link to p53 will certainly focus a great deal of attention on the CCT/cancer connection. Interestingly, recent evidence shows that many of the CCT subunits are overexpressed cancer.